

# Journal of Biomedical Optics

[SPIEDigitalLibrary.org/jbo](http://SPIEDigitalLibrary.org/jbo)

## **Near-infrared fluorescence imaging of experimentally collagen-induced arthritis in rats using the nonspecific dye tetrasulfocyanine in comparison with gadolinium-based contrast-enhanced magnetic resonance imaging, histology, and clinical score**

Ines Gemeinhardt  
Dorothee Puls  
Ole Gemeinhardt  
Matthias Taupitz  
Susanne Wagner  
Beatrix Schnorr  
Kai Licha  
Michael Schirner

# Near-infrared fluorescence imaging of experimentally collagen-induced arthritis in rats using the nonspecific dye tetrasulfocyanine in comparison with gadolinium-based contrast-enhanced magnetic resonance imaging, histology, and clinical score

Ines Gemeinhardt,<sup>a</sup> Dorothee Puls,<sup>a\*</sup> Ole Gemeinhardt,<sup>at</sup> Matthias Taupitz,<sup>a</sup> Susanne Wagner,<sup>a</sup> Beatrix Schnorr,<sup>a</sup> Kai Licha,<sup>b</sup> Michael Schirner,<sup>b</sup> Bernd Ebert,<sup>c</sup> Diethard Petzelt,<sup>c</sup> Rainer Macdonald,<sup>c</sup> and Jörg Schnorr<sup>a\*</sup>

<sup>a</sup>Charité-Universitätsmedizin Berlin, Department of Radiology, Campus Charité Mitte, Charitéplatz 1, 10117 Berlin, Germany

<sup>b</sup>mivenion GmbH, Robert-Koch-Platz 4, 10115 Berlin, Germany

<sup>c</sup>Physikalisch-Technische Bundesanstalt, Abbestraße 2–12, 10587 Berlin, Germany

**Abstract.** Using 15 rats with collagen-induced arthritis (30 joints) and 7 control rats (14 joints), we correlated the intensity of near-infrared fluorescence (NIRF) of the nonspecific dye tetrasulfocyanine (TSC) with magnetic resonance imaging (MRI), histopathology, and clinical score. Fluorescence images were obtained in reflection geometry using a NIRF camera system. Normalized fluorescence intensity ( $I_{NF}$ ) was determined after intravenous dye administration on different time points up to 120 min. Contrast-enhanced MRI using gadodiamide was performed after NIRF imaging. Analyses were performed in a blinded fashion. Histopathological and clinical scores were determined for each ankle joint.  $I_{NF}$  of moderate and high-grade arthritic joints were significantly higher ( $p < 0.005$ ) than the values of control and low-grade arthritic joints between 5 and 30 min after TSC-injection. This result correlated well with post-contrast MRI signal intensities at about 5 min after gadodiamide administration. Furthermore,  $I_{NF}$  and signal increase on contrast-enhanced MRI showed high correlation with clinical and histopathological scores. Sensitivities and specificities for detection of moderate and high-grade arthritic joints were slightly lower for NIRF imaging (89%/81%) than for MRI (100%/91%). NIRF imaging using TSC, which is characterized by slower plasma clearance compared to indocyanine green (ICG), has the potential to improve monitoring of inflamed joints.

© 2012 Society of Photo-Optical Instrumentation Engineers (SPIE). [DOI: 10.1117/JBO.17.10.106008]

Keywords: fluorescence imaging; rat; arthritis; magnetic resonance imaging; histopathology; experimental study.

Paper 12258 received May 2, 2012; revised manuscript received Aug. 29, 2012; accepted for publication Aug. 31, 2012; published online Oct. 1, 2012.

## 1 Introduction

Inflammatory joint diseases such as rheumatoid arthritis (RA) are common and have important economic implications.<sup>1,2</sup> Timely and affordable diagnosis is crucial for the patient's prognosis and therapeutic approach because early initiation of therapy can significantly delay the process of joint destruction.<sup>3,4</sup>

The diagnosis of inflammatory joint disease is currently based on the patient's history, clinical findings, laboratory results, and conventional radiography. The latter is not very sensitive in detecting early inflammatory changes of joints.<sup>5,6</sup> The early diagnosis has been much improved by supplementary imaging modalities such as skeletal scintigraphy, computed tomography (CT), arthrosonography, and magnetic resonance imaging (MRI)<sup>7</sup>; however, these modalities are not the first choice for routine use because they involve either radiation exposure or the examination is time-consuming and expensive.

A screening test that is both sensitive and inexpensive would be highly desirable for early detection of inflammatory disease and for treatment monitoring in patients. A promising candidate for this purpose is near-infrared fluorescence (NIRF) imaging. NIRF images contain information about optical properties of tissue such as reflection, absorption (e.g., by melanin and hemoglobin), and scattering (e.g., by cells, cell organelles, and collagen). Phantoms of finger joints have been developed to study optical properties related to early inflammatory changes by NIR imaging without dye administration.<sup>8,9</sup> In these studies, absorption coefficients and scattering coefficients were determined for healthy and abnormal synovial fluid and the joint capsule. Subsequently, an imaging technique called sagittal laser optical tomography (SLOT) has been developed, which yields transmission profiles of the finger joints and allows reconstruction of tomographic images of the sagittal finger plane.<sup>10–12</sup> It has been shown that this technique allows the identification of individual inflamed joints in patients with synovitis.<sup>13</sup> A drawback of this approach is the time-consuming acquisition and reconstruction of data and the marked variation of scattering and absorption in healthy volunteers.

The application of NIRF dyes may improve the diagnostic outcome of fluorescence imaging<sup>14</sup> as known for contrast-

\*Present address: University Medicine Greifswald, Institute of Diagnostic Radiology and Neuroradiology, Ferdinand-Sauerbruch-Straße 1, 17475 Greifswald, Germany.

<sup>†</sup>Present address: Freie Universität Berlin, Institute of Veterinary Anatomy, Faculty of Veterinary Medicine, Koserstraße 20, 14195 Berlin, Germany.

Address all correspondence to: Ines Gemeinhardt, Charité—Universitätsmedizin Berlin, Campus Charité Mitte, Department of Radiology, Charitéplatz 1, 10117 Berlin, Germany. Tel: +49 30 450 539 005; Fax: +49 30 450 527 993; E-mail: [ines.gemeinhardt@charite.de](mailto:ines.gemeinhardt@charite.de).

enhanced MRI.<sup>15</sup> Both specific<sup>16–20</sup> and nonspecific<sup>21–23</sup> fluorescent dyes have been investigated in animal models to test their potential for the detection of inflammation, e.g., in arthritis.<sup>22</sup> A promising nonspecific dye is tetrasulfocyanine (TSC), a modified cyanine dye which was already successfully used for *in vivo* imaging of subcutaneously growing tumors in animals.<sup>23</sup> Clinical trials are under way to investigate different nonspecific NIRF dyes for the visualization of arthritis<sup>24–26</sup> and superficial tumors, e.g., in optical mammography.<sup>27–29</sup>

TSC was selected for our experimental investigation because this dye exhibits increased hydrophilicity and less plasma protein binding, and therefore may possess improved imaging properties compared with ICG. Moreover, a higher fluorescence quantum yield (10%) in aqueous media has been reported for TSC compared with ICG (3%).<sup>23,30</sup>

To underpin the selection of TSC, we measured the concentrations of TSC and ICG in the eye over time using three control animals for each dye (unpublished results). This approach is not as accurate as measurement in pure blood, but for comparison of two dyes under the same experimental conditions, it might be acceptable since the eyes are nearly transparent. The blood half lives determined in this way were  $3.3 \pm 0.6$  min for ICG and  $31.7 \pm 1.5$  min for TSC. Measurements of normalized fluorescence intensity ( $I_{\text{NF}}$ ) of the joints of these control animals showed an eight times higher  $I_{\text{NF}}$  between 5 and 10 min after the injection of TSC compared to ICG.

Therefore, TSC is a promising contrast agent with improved optical and pharmacokinetic properties.

To our knowledge no study is available performing contrast-enhanced nonspecific fluorescence imaging and contrast-enhanced MRI with histological validation on the same animal.

It was hypothesized that: 1. NIRF imaging using the nonspecific dye TSC detects inflammation in an animal model of experimental arthritis and that 2. the NIRF intensity values correlate with the results of contrast-enhanced MRI, histopathology, and clinical evaluation.

## 2 Material and Methods

### 2.1 Animals and Arthritis Model

Animals were maintained in accordance with the Guide for the Care and Use of Laboratory Animals published by the US National Institute of Health (NIH publication No. 85–23, revised 1996), and examinations were approved by the responsible authority. Female Lewis rats (body weight 140 to 160 g) were purchased from Charles River Laboratories (Sulzfeld, Germany). The study was performed in 15 rats (30 joints) with collagen-induced arthritis (CIA) and seven control animals with healthy joints (14 joints).

For induction of CIA, bovine type II collagen (Collagen Acid Soluble, from Bovine Nasal Septum, Sigma–Aldrich Chemie GmbH, Steinheim, Germany) was dissolved in 0.01 M acetic acid. Subsequently, the solution was emulsified with an identical volume of incomplete Freund's adjuvant (Sigma–Aldrich Chemie GmbH, Steinheim, Germany) for 30 min in a well-closed container placed in an ultrasonic bath (35 kHz) (Sonorex RK 31, Bandelin, Berlin, Germany) filled with ice water.

For collagen injection the rats were immobilized by inhalation anesthesia with 2% isoflurane (Forene, Abbott GmbH, Wiesbaden, Germany) and medical oxygen. A dorsal area at the base of the tail was shaved and the skin disinfected. In 15 rats,

0.5 ml (containing 0.5 mg collagen) of the emulsion was intracutaneously injected at the base of the tail at different sites (each about 0.05 ml). The seven animals serving as controls were injected with 0.5 ml physiologic salt solution under identical conditions. The procedure was repeated in all rats after seven days.

Arthritis develops 13 to 15 days after the first collagen injection, but is highly variable in severity. Animals may show different degrees of arthritis in the right and left ankle joint, or there may be animals without signs of clinical or histological changes in one or both joints.

### 2.2 Clinical Evaluation (Score)

After the second collagen injection, the rats gait and the distal joints, especially the tibiotarsal joints, were inspected for swelling and reddening daily for describing the developing of arthritis. Before NIRF imaging each ankle joint was given a score from 0 to 3 (0 = no clinical symptoms, 1 = mild swelling, 2 = moderate swelling, and 3 = severe swelling with reduced mobility of the tibiotarsal joint).

### 2.3 NIRF Imaging

NIRF imaging of ankle joints was performed at the onset of clinical symptoms of arthritis. For examination, the rats were anesthetized by a combination of inhalation and injection anesthesia. First they were immobilized with isoflurane followed by subcutaneous injection of 80 mg/kg ketamine hydrochloride (Curamed Pharma GmbH, Karlsruhe, Germany) and 4 mg/kg xylazine (Rompun 2%, Bayer Vital GmbH, Leverkusen, Germany) in a mixing syringe and 3.5 mg/kg of diazepam (Diazepam ratiopharm 10 solution for injection, ratiopharm GmbH, Ulm, Germany) subcutaneously. An indwelling cannula (Vasocan Brauniüle, 0.9 mm diameter  $\times$  25 mm, B.Braun AG, Melsungen, Germany) was placed in the tail vein (lateral coccygeal vein) and connected with an automatic injector (P4000, IVAC/Alaris Medical Systems Inc., San Diego, USA) for the dye injection. The rats were placed in prone position and the hind legs extended caudolaterally. Hair was not removed since the ankle region is nearly not covered by fur and any manipulation that might induce hyperemia should be avoided.

Fluorescence images were obtained in reflection geometry. NIR dye fluorescence was excited with an optical parametric oscillator (OPO) (GWU-Lasertechnik, Erfstadt, Germany) based on an optically nonlinear BaB<sub>2</sub>O<sub>4</sub>-crystal, pumped by the third harmonic ( $\lambda = 355$  nm,  $E_{\text{pulse}} = 80$  mJ) of a Q-switched Nd:YAG laser (GCR–10, Spectra-Physics Inc., USA). The OPO provides laser radiation tuneable between 415 nm and 2.2  $\mu$ m and was set to  $\lambda_{\text{ex}} = 740$  nm in our experiments to excite NIR fluorescence of the dye under investigation. Two long-pass interference filters ( $\lambda_{50\%} = 800$  nm) and a long-pass edge filter ( $\lambda_{50\%} = 780$  nm, 3 mm) were used to cut off scattered excitation light from emitted fluorescence light. The cut-off wavelength at  $\lambda = 860$  nm results from a sensitivity drop of the detector. The fluorescence was imaged onto the photocathode of a water/Peltier-cooled, intensified CCD camera (Model ICCD-576, Princeton Instruments Inc, Trenton, USA) with the help of a standard object lens of 50 mm focal length ( $f = 1.4$ ). In order to suppress background signals caused by ambient light, the intensifier of the CCD camera was gated applying an electrical pulse ( $-180$  V) of about 10 ns duration derived from a HV pulse generator. The HV pulse generator was

synchronized with an advanced trigger pulse provided by the power supply of the laser system and appropriately delayed by means of a digital delay generator. The delay of the gating pulse was adjusted to image the fluorescence of the cyanine dye (decay time  $\sim 300$  ps) and to suppress long-living autofluorescence components with typical decay times of 3 ns. Fluorescence was recorded using a short exposure time (0.2 s) and 4 times accumulation to avoid motion artifacts. For close monitoring of dye uptake immediately after injection, 180 images were recorded within 660 s (i.e., one image every 3.65 s), followed by time points at 30, 60, and 120 min post injection.

A stable fluorescent cube consisting of covalently bound cyanine dyes embedded in plastic material placed in the top right corner of the measuring field served as reference for fluorescence intensity.

## 2.4 NIRF Dye

The nonspecific NIRF dye, TSC, is a tetrasulfonated carbocyanine dye based on an indotricarbocyanine chromophore. TSC is a low-molecular-weight dye (836.9 g/mol) with both anionic and hydrophilic properties.<sup>23,30</sup> In phosphate-buffered saline TSC shows an absorption maximum at  $\lambda_{\text{abs}} = 755$  nm and a fluorescence emission maximum at  $\lambda_{\text{em}} = 778$  nm.<sup>23</sup> TSC has a plasma binding of about 74% and in rats excretion is mostly (70%) hepatobiliary in feces.<sup>23</sup> The dye was dissolved in physiological saline and injected as an intravenous bolus into the tail vein at a dose of 1  $\mu\text{mol/kg}$  and a rate of 4 ml/min. The fluorescent contrast agent was administered at the start of the third frame.

## 2.5 NIRF Imaging Data Analysis

The acquired data were transferred to a desktop computer and stored. The first two frames of the sequence served as background frames. Circular regions of interest (ROIs) with a constant diameter of 20 pixels were placed over the reference cube in the top right corner and the left and right ankle joints with the center of the ROI positioned over the external malleolus by one reader (BE) blinded to MRI results, histopathological and clinical grading.

Mean fluorescence intensities  $I_F$  were the average of all fluorescence intensity values of pixels covered by the ROI of a particular region under investigation divided by the number of pixels. All fluorescence intensities were normalized ( $I_{\text{NF}}$ ) to the fluorescence of the reference mean  $I_F(\text{reference})$  to obtain relative values using the following equation:

$$I_{\text{NF}} = I_F(\text{joint})/I_F(\text{reference}), \quad (1)$$

where  $I_{\text{NF}}$  is the normalized fluorescence intensity,  $I_F(\text{joint})$  is the mean fluorescence intensity over the ankle joint, and  $I_F(\text{reference})$  is the mean fluorescence intensity of the reference.

Contrast enhancement was determined by calculating  $I_{\text{NF}}$  at 5 and 10 min after dye administration and additionally after 30, 60, and 120 min.

## 2.6 MR Imaging

The rats were examined 5 h after NIRF imaging on a 1.5 T whole-body MR scanner (Magnetom Sonata, Siemens, Erlangen, Germany) using an extremity coil (Siemens, Erlangen,

Germany). The rats were placed in prone position with the hind legs extended caudolaterally on a Styrofoam support and positioned on a horizontal line in the center of the coil. MR images were acquired with a T1-weighted spin-echo (SE) sequence in coronal slice orientation using the following sequence parameters: echo time 13 ms, repetition time 350 ms, field of view  $160 \times 144$  mm<sup>2</sup>, matrix  $173 \times 320$ , slice thickness 2 mm, and number of slices 13. The total acquisition time was 4 min and 13 s.

Following acquisition of nonenhanced MR images, the gadolinium-based contrast agent gadodiamide (Omniscan, Amersham Buchler GmbH & CO. KG, Braunschweig, Germany) was injected as a bolus into the tail vein at a dose of 0.2 mmol Gd/kg. Acquisition of contrast-enhanced images was started at the same slice position about 3 min after administration of contrast agent.

Due to the start of image acquisition about 3 min after contrast medium administration and the acquisition time, the MRI data values were identified as 5 min value.

## 2.7 Analysis of MR Images

MRI always has a morphologic background; therefore, it is necessary to include the precontrast signal intensity in analyzing MRI contrast medium enhancement. The MR images were analyzed by one reader (DP) blinded to time point of acquisition, NIRF imaging findings, histopathological, and clinical scores. The reader determined relative signal intensities (SI) [signal-to-noise ratio (SNR)] in the ankle joints before and after administration of contrast agent using the software ImageJ (National Institutes of Health, Maryland, USA). SI of the left and right ankle joints were measured in circular ROIs with a constant diameter and the center positioned in the same way as for analysis of NIRF images. SI of the background was measured outside the animal. SNRs of the ankle joints before ( $\text{SNR}_{\text{pre}}$ ) and after contrast enhancement ( $\text{SNR}_{\text{post}}$ ) were calculated as ratios of SI in the joints to background intensities. The percent signal intensity increase ( $\Delta\text{SI}\%$ ) in ankle joints after contrast enhancement was then calculated according to the following formula:

$$\Delta\text{SI}\% = (\text{SNR}_{\text{post}} - \text{SNR}_{\text{pre}})/\text{SNR}_{\text{pre}} \times 100. \quad (2)$$

## 2.8 Histology

The animals were euthanized in deep anesthesia by intravenous injection of T61 ad us. vet. (Intervet Deutschland GmbH, Unterschleißheim, Germany) at a dose of 2 ml/animal immediately after MRI.

For histological workup, the hind legs of the animals were removed and fixed in 4% buffered formaldehyde solution (Mallinckrodt Baker, Deventer, Holland). Subsequently, the specimens were placed in EDTA decalcifying solution (Herbeta Arzneimittel, Berlin, Germany) for 5 weeks at 60°C. The solution was changed every week. The decalcified hind legs were embedded in paraffin, thereafter about 4- $\mu\text{m}$  thick histological sections were cut and stained with hematoxylin and eosin (H&E).

The histopathological specimens (Fig. 1) were assessed for signs of arthritis using the following criteria: synovitis, peri-arthritis, tenosynovitis, periostitis, and cartilage/bone destruction. Each criterion was graded semiquantitatively with predetermined parameter values by one reader (IG) blinded to NIRF and MRI values as well as clinical score on the basis of a

standardized human synovitis scale,<sup>31</sup> which distinguishes four degrees of severity: 0 (absence of criterion), 1 (mild), 2 (moderate), and 3 (severe). The sum score was graded as follows: 0, no arthritis; 1 to 5, low-grade arthritis; 6 to 10, moderate arthritis; and 11 to 15 high-grade arthritis.

## 2.9 Statistical Analysis

To compare different groups the medians (50th percentile) were calculated and tests of descriptive statistics were used.

For analysis of NIRF and MRI data, the whole group of animals with arthritis and the control group were tested for significant differences in  $I_{NF}$ , signal intensity, and signal increase at different time points given in minutes (NIRF: 5, 10, 30, 60, 120; MRI: 5). Additionally, the animals with arthritis were classified into three different groups (low-grade, moderate, and high-grade) based on histopathological scores. SI and signal increases, respectively, of both imaging modalities were compared between these subgroups and with controls at time points given above. Differences between any two CIA groups or controls were tested for significance using the nonparametric Mann-Whitney U-test. Significance was assumed at  $p < 0.05$ . Differences in  $I_{NF}$  at different time points and differences in signal increases between all CIA groups and controls were tested for significance using the nonparametric Kruskal-Wallis analysis. A very highly significant difference was assumed at  $p < 0.001$ , a highly significant difference at  $p < 0.01$ .

Associations between clinical parameters, histology, and the two imaging modalities were identified by calculating Spearman correlation coefficients ( $r_s$ ). Significance was assumed at  $p < 0.05$ . Statistical tests were performed using SPSS version 13.0 (SPSS Inc., Chicago, USA).

Sensitivity and specificity for the detection of arthritic joints were calculated. Sensitivity gives the percentage of correctly identified arthritic joints (number of arthritic joints with NIRF value higher than discriminator related to number of all arthritic joints). Specificity measures the proportion of healthy joints correctly identified by NIRF imaging (number of control

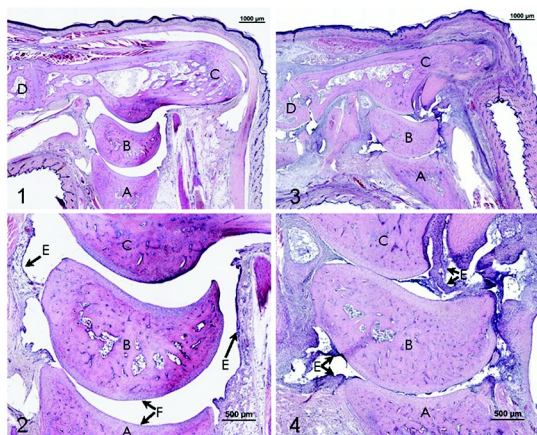


**Fig. 1** H&E-stained histological sections of a control joint (left, 1 and 2) and an arthritic joint (right, 3 and 4). 1 and 3: (1) Overview of a tibiotarsal joint in a control rat and (3) in an arthritic joint showing (A) tibia, (B) talus, (C) calcaneus, and (D) tarsal bone. 2: Detail of tibiotarsal joint in a control animal showing (E) the joint space with synovial membrane and (F) the articular cartilage. 4: Detail of tibiotarsal joint of an arthritic joint showing (E) proliferating synovial membrane filling the joint space and covering the destroyed cartilage.

joints with NIRF value lower than discriminator related to number of all control joints).

ROC curve analysis was used to calculate the cut-off value with the highest number of samples correctly classified (true positives plus true negatives).

$I_{NF}$  at the different time points were graphically represented in box-and-whisker plots. Outliers are indicated by open circles, extremes by asterisks.

## 3 Results

### 3.1 NIRF Imaging

In pre-injection NIRF images, both control joints and arthritic joints showed very low  $I_{NF}$  (0.045 and 0.05) without differences between the groups.

Five minutes after dye administration, all  $I_{NF}$  values were significantly higher than the corresponding intensities before administration ( $p < 0.05$ ), regardless of the degree of arthritis.

The  $I_{NF}$  of control joints and joints from CIA rats were compared. The group of arthritic joints showed statistically significant higher  $I_{NF}$  values than the control joints 5, 10, 30, and 60 min after dye administration ( $p < 0.05$ ). The difference in  $I_{NF}$  between the group of arthritic joints and controls was no longer significant after 120 min (Figs. 2 and 3).

In all three arthritis subgroups, the highest  $I_{NF}$  was found 5 and 10 min after dye administration. The highest ratio of median

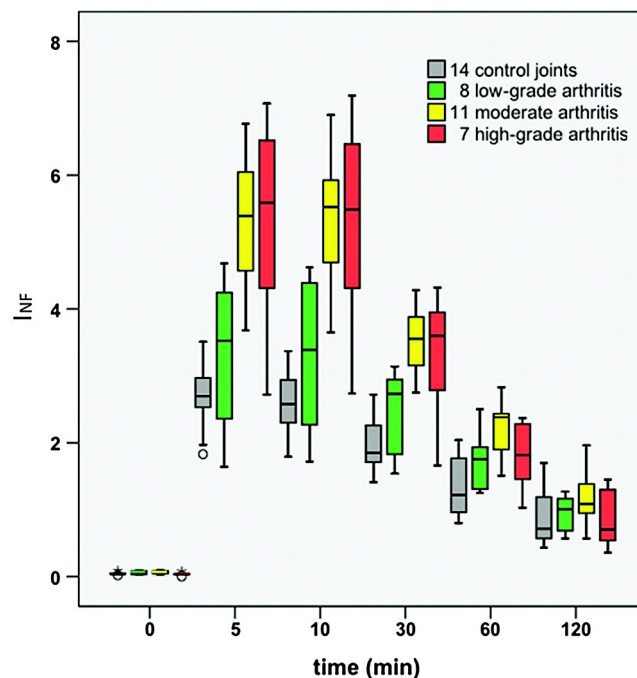


**Fig. 2** Box-and-whisker plots of normalized fluorescence intensities  $I_{NF}$  for all groups of joints investigated at different time points. The  $I_{NF}$  values of the joints with moderate and high-grade arthritis are markedly above the values of the control joints between 5 and 60 min after dye injection ( $p < 0.05$ ). The  $I_{NF}$  values of joints with low-grade arthritis are only slightly above those of the controls ( $p > 0.05$ ). The difference in  $I_{NF}$  values between the three grades of arthritis is especially pronounced 5 min after dye administration. The differences between all groups were very highly significant between 5 and 30 min after dye administration ( $p < 0.001$ ), highly significant at 60 min ( $p = 0.001$ ), and nonsignificant at 120 min and before dye administration. Outliers are denoted by open circles, extremes by asterisks.

$I_{NF}$  of all arthritic joints to all control joints was obtained 10 min after dye administration [median  $I_{NF}(\text{arthritis})/\text{median } I_{NF}(\text{control}) = 4.76/2.58 = 1.84$ ]. The relative fluorescence intensity showed a marked decrease for all groups at 30 min and a further decrease at 120 min after dye administration (Fig. 2).

In more detail, the median  $I_{NF}$  of the animals with low-grade arthritis was above those of the controls at all time points (Fig. 2), but the difference was not statistically significant. Furthermore, there is no significant difference between moderate and high-grade arthritis to all time points.

In contrast, the median  $I_{NF}$  of animals with moderate arthritis and the ones with high-grade arthritis differ significantly from those of animals with no or with low-grade arthritis for all time points except for 120 min (Fig. 2). The highest ratio (2.14) between the median  $I_{NF}$  of moderate and high-grade arthritis joints versus the median  $I_{NF}$  of controls was reached 10 min after dye administration.

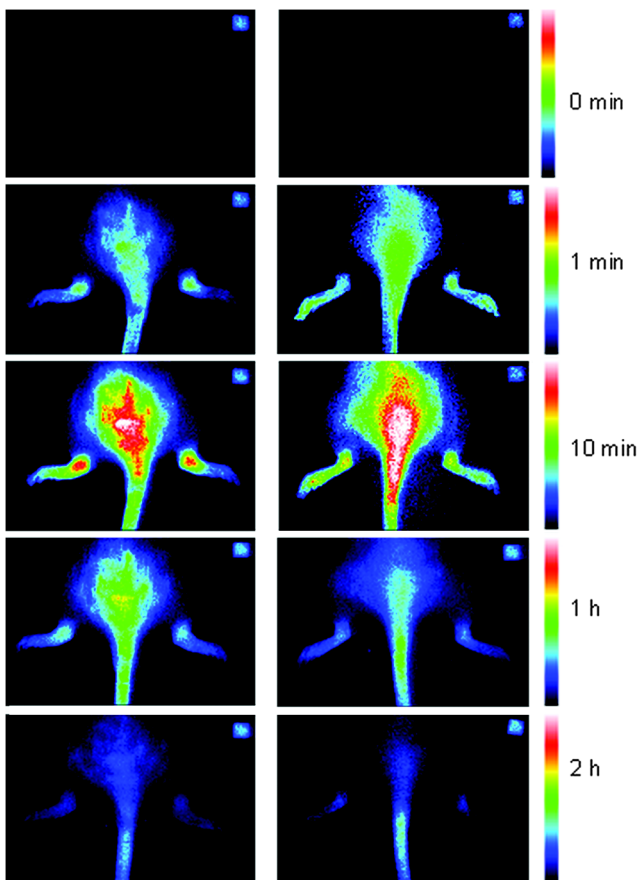


**Fig. 3** Fluorescence images in false colors (range 0 to 100,000 counts for all color bars) before and after administration of  $1 \mu\text{mol/kg}$  TSC. The time course is shown in a rat with high-grade CIA on the left and a healthy control rat on the right. The fluorescent cube used as reference is seen in the upper right corner of the images. Red color (high fluorescence intensity) indicates areas of inflammation. The high signal intensities in the back region are caused by shaving and skin inflammation due to the intradermal injections. The hot spots in the ankle joints of the CIA rat (left) 1 and 10 min after injection clearly indicate arthritis, while the control joints (right) appear homogeneous. The fluorescence intensities decrease with the time elapsed since dye injection. Two hours after injection there is only very weak relative fluorescence intensity visible.

Kruskal-Wallis analysis was used to test differences between the three groups (low-grade, moderate, and high-grade) and controls at different time points after dye administration. Very highly significant differences ( $p < 0.001$ ) were seen 5, 10, and 30 min after dye administration; no significant differences were found before and 120 min after dye administration.

Using the relative fluorescence intensities of all groups determined at 5 min and 10 min after dye administration in ROC curve analysis we identified 3.07 at 5 min and 3.15 at 10 min as the cut-off values with the highest numbers of samples correctly classified (85%). Using these values, we achieved a sensitivity of 84.6% and specificity of 85.7% at both time points.

Using the discriminator of 3.5 at 5 and 10 min after dye administration, the calculated sensitivity was 77% for both time points, while specificity was 93% and 100%, respectively, for classifying a joint as arthritic regardless of arthritis grades. Using the same discriminator for joints with moderate and high-grade arthritis, sensitivity was 89% with specificity of 81% and 85%, respectively.

With use of a higher discriminator, specificity increases while sensitivity decreases. For instance, with a discriminator of 5, moderate or high-grade arthritis is detected with a specificity of 100% at 5 and 10 min while sensitivity is only 67%.

### 3.2 MR Imaging

In pre-injection MR images, there were significant differences in SI between control joints and the group of all arthritic joints ( $p < 0.05$ ) but no significant differences in SI between low-grade, moderate, and high-grade arthritis.

Five minutes after administration of the contrast agent, MRI SNRs were significantly higher than the corresponding intensities before administration ( $p < 0.05$ ) regardless of the degree of arthritis.

The group of all arthritic ankle joints had higher SNR on post-contrast images than the control group (Fig. 4), and the percentage signal increase was also significantly higher.

The post-contrast SNR and the percentage signal increase in rats with low-grade arthritis did not differ significantly from controls. Moderate and high-grade arthritic joints differed significantly from low-grade arthritic joints and controls (Fig. 5).

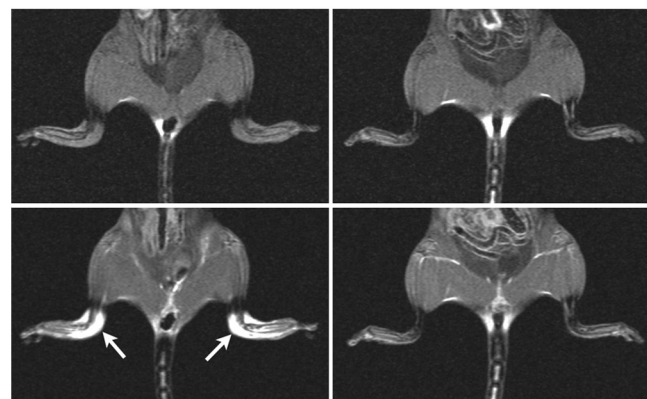


**Fig. 4** T1-weighted spin echo MR images of the ankle joints in a rat with bilateral high-grade arthritis (left) and a control (right). Upper row: before administration of contrast agent; lower row: after administration of contrast agent. There is marked enhancement in the area of the ankle joints in the rat with high-grade arthritis (arrows) while there is no signal increase after administration of contrast agent in the control rat.

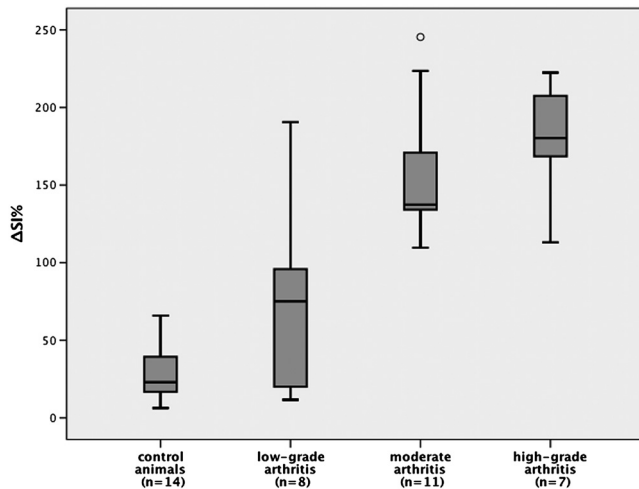


**Fig. 5** Increase in  $\Delta SI\%$  in controls and the three arthritis groups. Kruskal-Wallis analysis yielded very highly significant differences ( $p < 0.001$ ) between all groups. The  $\Delta SI\%$  values in moderate and high-grade arthritis are markedly higher than in low-grade arthritis and control animals. The values  $\Delta SI\%$  of the rats with low-grade arthritis are only slightly higher than the values of the control animals. The open circle indicates an outlier.

Kruskal-Wallis analysis yielded a very highly significant difference ( $p < 0.001$ ) in  $\Delta SI\%$  between the three arthritis groups and controls.

The  $\Delta SI\%$  of 59 is the cut-off value with the highest number of samples correctly classified (87.5%). This cut-off yielded 88.5% sensitivity and 85.7% specificity.

Using the discriminator of  $\Delta SI\%$  80 at 5 min after administration, we calculated a sensitivity of 77% and a specificity of 100%, respectively, for classifying a joint as arthritic regardless of arthritis grade.

It is worth noting that there is no significant difference between moderate and high-grade arthritis in terms of post-contrast SNR or percent signal increases. The sensitivity and specificity for the groups of high-grade and moderate arthritis are 100% and 91%, respectively, when using  $\Delta SI\% = 80$  as discriminator between controls and inflamed joints.

### 3.3 Histology

For comparative analysis of  $I_{NF}$  (NIRF) and SNR (MRI), histology was performed for joints with collagen injection (30 joints in 15 animals) and for controls (14 joints in 7 animals).

None of the 14 control joints showed histologic evidence of arthritis.

In the group with collagen injection (30 joints), four joints in four different animals did not develop arthritis and were excluded from statistical analysis.

In the remaining 26 joints, which developed histologic changes after collagen-injection, the changes were classified as low-grade arthritis in eight joints, moderate arthritis in eleven joints, and high-grade arthritis in seven joints.

### 3.4 Clinical Findings

There were no clinical signs of arthritis in any of the 7 control animals (14 joints).

In the animals with collagen injection, we observed initial clinical symptoms in the form of unilateral or bilateral swelling

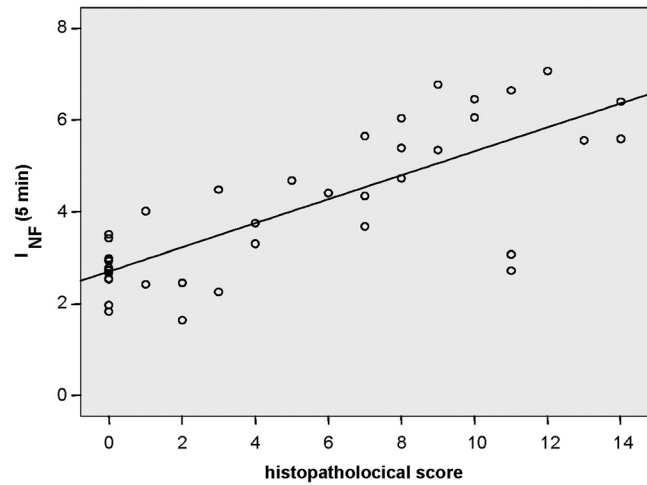


**Fig. 6** Scatter diagram of the correlation between normalized fluorescence intensity of the ankle joint 5 min after injection of TSC versus the histopathological score ( $r_s = 0.74$ ,  $p < 0.001$ ).

of the ankle joints on days 13 to 15 after the first collagen injection. Out of 30 joints from 15 animals, 7 joints showed no clinical symptoms, 4 joints showed mild swelling, 6 joints moderate swelling, and 13 joints severe swelling.

### 3.5 Correlation

Relative fluorescence intensity  $I_{NF}$  5 min after dye administration showed high correlation with both the histopathological scores ( $r_s = 0.742$ ) (Fig. 6) and the clinical scores ( $r_s = 0.741$ ) of the individual joints. The percentage signal increase on MRI also correlated well with the histopathological and clinical scores ( $r_s = 0.816$ ,  $r_s = 0.761$ ). Correlations were also high for the two imaging modalities, NIRF and MRI ( $r_s = 0.685$ ), as well as for clinical and histological assessment of arthritis ( $r_s = 0.874$ ).

## 4 Discussion

The synovial membrane of patients with arthritis such as RA is characterized by hyperplasia, increased vascularization, and invasion of inflammatory cells.<sup>32</sup> These early inflammatory changes of soft tissue are more sensitively detected by scintigraphy, ultrasound (US), and MRI than conventional radiography.<sup>5,7</sup> Scintigraphy is very sensitive but unspecific and is primarily used for early diagnosis and evaluation of the pattern of involvement. It is unsuitable for routine use and follow-up examinations because of the radiation exposure and the high costs.<sup>33</sup> US allows the evaluation of periarticular soft tissue<sup>34</sup> and the identification of small superficial bone erosions.<sup>35,36</sup> Various studies have shown that Doppler US is a sensitive tool for the detection of active synovitis.<sup>37-39</sup> Major limitations of US are that the results crucially rely on the examiner's experience<sup>33,40</sup> and that the examination and documentation of the findings are time consuming. Contrast-enhanced MRI also demonstrates synovial hyperemia before destructive lesions of the cartilage and bone occur<sup>41</sup> and monitors synovial proliferation and joint effusions.<sup>5</sup> However, the routine use of MRI is limited by the fact that it is time consuming and expensive.

Dye-enhanced NIRF imaging might be a promising modality for such a routine checkup.

Nonspecific fluorescent dyes that have been investigated before in animal models include both agents with predominantly intravascular distribution (e.g., indocyanine green, ICG) and agents with higher extravasation into tissue (e.g., SIDAG).<sup>42</sup> It has been reported that the signal enhancement of nonspecific optical contrast agents (e.g., ICG<sup>43</sup> or SIDAG<sup>25,44</sup>) is linearly correlated with tissue vascularization. Studies have shown that NIRF imaging using these nonspecific dyes has the potential for detection of inflammatory joints.<sup>24,26</sup>

In the current study we investigated the enhancement induced by the nonspecific NIRF dye TSC in ankle joints of rats with CIA. TSC is a well-tolerated cyanine dye of similar chemical nature as ICG; however, its *in vivo* properties (plasma binding, circulation time) are different from those of ICG.<sup>23</sup> Having lower protein binding than ICG, TSC may extravasate, and elimination from blood circulation by liver uptake is not as rapid as for ICG.<sup>23</sup> These properties could permit a more efficient leakage into inflamed vascular spaces.

NIRF imaging using nonspecific TSC enables differentiation of arthritic joints from normal joints by means of an increase in relative fluorescence intensity,  $I_{NF}$ , which correlates with the severity of arthritis (Fig. 6). The markedly higher signal increase in joints with moderate and high-grade arthritis as opposed to low-grade inflammatory changes suggests that more severe inflammation causes a higher fluorescence signal due to tissue vascularization and possibly an increased extravasation of the dye. The time course of TSC accumulation was found to be similar in all groups investigated.  $I_{NF}$  was highest 5 and 10 min after dye administration both in arthritic rats and healthy animals. A continuous decrease in  $I_{NF}$  in all groups investigated was seen until 2 h after injection due to hepatic elimination of the dye. The observed time course of fluorescence intensities in arthritic ankle joints is similar to the course described by Perlitz et al. in tumor-bearing rats.<sup>23</sup> They found fluorescence intensity to be highest 10 to 20 min after TSC injection with a subsequent decrease.<sup>23</sup>

High correlation between near-infrared SI and clinical arthritis scores was also found by Izmailova et al.<sup>45</sup> using specific probes in an animal model. Dyes with molecular specificity used for arthritis detection and monitoring of therapy by other study groups such as protease-activated dyes,<sup>18,45,46</sup> fluorescence-labeled folate probes,<sup>16</sup> and dyes coupled to antibodies<sup>17</sup> result in higher contrast in inflammatory areas compared to normal controls. These results indicate how the method may be improved in the future. However, the allergic potential of these dyes, slow accumulation in tissue, as well as issues of chemical development, such as the complicated manufacturing process, prolong the route to possible clinical application. Moreover, the usefulness in terms of workflow in the routine clinical setting might be advantageous with blood pool probes providing more rapid diagnostic results.

An important advantage of the NIRF imaging method presented here might be the use of a nonspecific, highly biocompatible dye, and the availability of a series of whole-body images of the rat with a frame rate of about 5 images/s, as well as the simple analysis compared to other evaluation procedures based on scattering and absorption data for assessment of finger joints.<sup>10,11,13,47</sup>

T1-weighted contrast-enhanced MRI was performed to compare the degree of contrast enhancement with NIRF imaging. To this end MRI was performed with gadolinium-based contrast agent like use in clinical setting for imaging of arthritic finger joints.<sup>41,48</sup>

For comparison of NIRF and MRI data, the values at 5 min were used because joint contrast has been reported to increase dramatically about 4 to 5 min after injection of gadolinium-based MRI contrast agent injection in knees of rats with monoarticular arthritis.<sup>49</sup>

In contrast to NIRF imaging, MRI signal intensities determined in animals with moderate and high-grade arthritis already differ from the SI in control animals before administration of contrast agents. The signal changes in MR images of arthritic joints are due to pathologic processes induced by inflammation.<sup>50,51</sup> Acute arthritis as in the rats investigated here begins with joint effusion. These changes in perfusion and permeability associated with inflammation result in an increase of T2 relaxation times.<sup>15</sup> In addition to joint effusion, inflammation is associated with edema of the synovial membrane, which also affects the MRI signal. The synovial changes associated with low-grade arthritis are too small to cause a statistically significant SI increase in MR images. The calculation of the difference in SI in % after administration of gadodiamide improves the differentiation between joints with low-grade arthritis and control joints compared to absolute SI values; however, the difference is not significant ( $p = 0.06$ ).

Following contrast administration, there is an increase in signal intensity with both modalities that correlates with the severity of arthritis. Comparison of the groups reveals no significant differences between contrast-enhanced NIRF imaging and MRI.

The absence of differences in MR and NIRF imaging between moderate and high-grade arthritis suggest that advanced inflammation with hyperplasia of the synovial membrane, fibroplasia, and pannus formation does not induce further accumulation of nonspecific contrast media in affected areas.

The specimens for histopathological analysis were obtained on the same day as NIRF and MR imaging were performed, thus representing the histopathological situation as close as possible to the time point of imaging. The specimens are therefore well suited to be used as gold standard for evaluation. Histopathological changes such as thickening of the synovial cover cell layer, invasion of inflammatory cells, connective tissue proliferation, and pannus formation correspond to findings reported in the literature.<sup>52-54</sup>

The animal model of CIA used in our study is characterized by articular changes that resemble RA in humans,<sup>52-54</sup> and CIA is induced by the same factors that cause human RA.<sup>55</sup>

A limitation is the lack of accurate blood half lives of TSC compared with ICG and of a direct comparison of ICG and TSC in experimental CIA in rats.

## 5 Conclusion

Our study demonstrates that contrast-enhanced NIRF imaging using the nonspecific dye TSC has a similar sensitivity as MRI using a nonspecific gadolinium-based contrast medium in differentiating inflamed joints from healthy joints in an experimental rat model. NIRF imaging, therefore, is a promising candidate for the early diagnosis of inflammatory joints. An advantage of the NIRF imaging method presented here is that it is affordable and can be performed within a short time.

The good correlation between  $I_{NF}$  and SI values and the clinical and histopathological scores indicate that NIRF imaging using TSC, similar to MRI using unspecific gadodiamide, can be used for assessing the degree of inflammation of arthritic joints. A nonspecific NIRF dye with similar properties as TSC

might be used for the diagnosis of arthritis and treatment monitoring in the clinical setting.

### Acknowledgments

This research was supported in part by the European Regional Development Fund (ERDF) and by the Investitionsbank Berlin (IBB). The authors thank Ms. Bettina Herwig for translating the manuscript.

### References

- J. Bernhard and P. M. Villiger, "Rheumatoid arthritis: pathogenesis and pathology," *Schweiz Med Forum* **8**, 179–183 (2001).
- S. Merkesdal et al., "Indirect medical costs in early rheumatoid arthritis: composition of and changes in indirect costs within the first three years of disease," *Arthritis Rheum.* **44**(3), 528–534 (2001).
- P. Emery, "Early rheumatoid arthritis: therapeutic strategies," *Scand. J. Rheumatol. Suppl.* **23**, 3–7 (1994).
- W. S. Wilke, T. J. Sweeney, and L. H. Calabrese, "Early, aggressive therapy for rheumatoid arthritis: concerns, descriptions, and estimate of outcome," *Semin. Arthritis Rheum.* **23**(2), 26–41 (1993).
- M. Backhaus et al., "Arthritis of the finger joints: a comprehensive approach comparing conventional radiography, scintigraphy, ultrasound, and contrast-enhanced magnetic resonance imaging," *Arthritis Rheum.* **42**(6), 1232–1245 (1999).
- A. C. Brower, "Use of the radiograph to measure the course of rheumatoid arthritis. The gold standard versus fool's gold," *Arthritis Rheum.* **33**(3), 316–324 (1990).
- A. Munding, E. Moser, and M. Langer, "Imaging in rheumatoid arthritis," *Immun. Infekt.* **21**(3), 64–68 (1993).
- J. Beuthan et al., "Initial studies of the application of the linear signal transfer theory in evaluating diaphanoscopy examinations exemplified by rheumatism diagnosis," *Biomed. Tech. (Berl.)* **46**(11), 298–303 (2001).
- V. Prapavat et al., "The development of a finger joint phantom for the optical simulation of early inflammatory rheumatic changes," *Biomed. Tech.* **42**(11), 319–326 (1997).
- A. H. Hielscher et al., "Near-infrared diffuse optical tomography," *Dis. Markers* **18**(5–6), 313–337 (2002).
- A. H. Hielscher et al., "Sagittal laser optical tomography for imaging of rheumatoid finger joints," *Phys. Med. Biol.* **49**(7), 1147–1163 (2004).
- A. K. Scheel et al., "Laser imaging techniques for follow-up analysis of joint inflammation in patients with rheumatoid arthritis," *Med. Laser Appl.* **18**(3), 198–206 (2003).
- A. K. Scheel et al., "First clinical evaluation of sagittal laser optical tomography for detection of synovitis in arthritic finger joints," *Ann. Rheum. Dis.* **64**(2), 239–245 (2005).
- T. Fischer et al., "Detection of rheumatoid arthritis using non-specific contrast enhanced fluorescence imaging," *Acad. Radiol.* **17**(3), 375–381 (2010).
- E. W. St Clair, D. S. Pisetsky, and B. F. Haynes, *Rheumatoid Arthritis*, 1st ed., Lippincott Williams & Wilkins, Philadelphia (2004).
- W. T. Chen et al., "Arthritis imaging using a near-infrared fluorescence folate-targeted probe," *Arthritis Res. Ther.* **7**(2), R310–R317 (2005).
- A. Hansch et al., "In vivo imaging of experimental arthritis with near-infrared fluorescence," *Arthritis Rheum.* **50**(3), 961–967 (2004).
- W. F. Lai et al., "Early diagnosis of osteoarthritis using cathepsin B sensitive near-infrared fluorescent probes," *Osteoarthritis Cartilage* **12**(3), 239–244 (2004).
- S. Vollmer et al., "Extra domain B fibronectin as a target for near-infrared fluorescence imaging of rheumatoid arthritis affected joints in vivo," *Mol. Imaging* **8**(6), 330–340 (2009).
- A. Wunder et al., "In vivo imaging of protease activity in arthritis: a novel approach for monitoring treatment response," *Arthritis Rheum.* **50**(8), 2459–2465 (2004).
- B. Ebert et al., "Cyanine dyes as contrast agents for near-infrared imaging in vivo: acute tolerance, pharmacokinetics, and fluorescence imaging," *J. Biomed. Opt.* **16**(6), 066003 (2011).
- R. Meier et al., "Indocyanine green-enhanced imaging of antigen-induced arthritis with an integrated optical imaging/radiography system," *Arthritis Rheum.* **62**(8), 2322–2327 (2010).
- C. Perlitz et al., "Comparison of two tricarbo-cyanine-based dyes for fluorescence optical imaging," *J. Fluoresc.* **15**(3), 443–454 (2005).
- S. G. Werner et al., "Inflammation assessment in patients with arthritis using a novel in vivo fluorescence optical imaging technology," *Ann. Rheum. Dis.* **71**(4), 504–510 (2012).
- C. Bremer, S. Werner, and H.-E. Langer, "Assessing activity of rheumatic arthritis with fluorescence optical imaging," *Eur. Musculoskeletal Rev.* **4**(2), 96–100 (2009).
- T. Dziekan et al., "Detection of rheumatoid arthritis by evaluation of normalized variances of fluorescence time correlation functions," *J. Biomed. Opt.* **16**(7), 076015 (2011).
- D. Grosenick et al., "Time-domain optical mammography: initial clinical results on detection and characterization of breast tumors," *Appl. Opt.* **42**(16), 3170–3186 (2003).
- A. Poellinger et al., "Breast cancer: early- and late-fluorescence near-infrared imaging with indocyanine green—a preliminary study," *Radiology* **258**(2), 409–416 (2011).
- A. Poellinger et al., "Near-infrared imaging of the breast using omocyanine as a fluorescent dye: results of a placebo-controlled, clinical, multicenter trial," *Invest. Radiol.* **46**(11), 697–704 (2011).
- K. Licha et al., "Hydrophilic cyanine dyes as contrast agents for near-infrared tumor imaging: synthesis, photophysical properties and spectroscopic in vivo characterization," *Photochem. Photobiol.* **72**(3), 392–398 (2000).
- V. Krenn et al., "Grading of chronic synovitis—a histopathological grading system for molecular and diagnostic pathology," *Pathol. Res. Pract.* **198**(5), 317–325 (2002).
- D. Isenberg et al., *Oxford Textbook of Rheumatology*, 3rd ed., Oxford University Press, New York (2004).
- R. J. Wakefield, W. W. Gibbon, and P. Emery, "The current status of ultrasonography in rheumatology," *Rheumatology* **38**(3), 195–198 (1999).
- M. Ostergaard and M. Szkudlarek, "Imaging in rheumatoid arthritis—why MRI and ultrasonography can no longer be ignored," *Scand. J. Rheumatol.* **32**(2), 63–73 (2003).
- M. Backhaus et al., "Technique and diagnostic value of musculoskeletal ultrasonography in rheumatology. Part 6: ultrasonography of the wrist/hand," *Z. Rheumatol.* **61**(6), 674–687 (2002).
- M. Szkudlarek et al., "Ultrasonography of the metacarpophalangeal and proximal interphalangeal joints in rheumatoid arthritis: a comparison with magnetic resonance imaging, conventional radiography and clinical examination," *Arthritis Res. Ther.* **8**(2), R52 (2006).
- E. Qvistgaard et al., "Quantitative ultrasonography in rheumatoid arthritis: evaluation of inflammation by Doppler technique," *Ann. Rheum. Dis.* **60**(7), 690–693 (2001).
- M. Szkudlarek et al., "Interobserver agreement in ultrasonography of the finger and toe joints in rheumatoid arthritis," *Arthritis Rheum.* **48**(4), 955–962 (2003).
- L. Terslev et al., "Doppler ultrasound and magnetic resonance imaging of synovial inflammation of the hand in rheumatoid arthritis: a comparative study," *Arthritis Rheum.* **48**(9), 2434–2441 (2003).
- R. Landewe and D. van de Heijde, "Is radiographic progression a realistic outcome measure in clinical trials with early inflammatory arthritis?," *Clin. Exp. Rheumatol.* **21**(5), S37–S41 (2003).
- M. Bollow et al., "Quantitative analyses of sacroiliac biopsies in spondyloarthropathies: T cells and macrophages predominate in early and active sacroiliitis—cellularity correlates with the degree of enhancement detected by magnetic resonance imaging," *Ann. Rheum. Dis.* **59**(2), 135–140 (2000).
- T. Fischer et al., "Assessment of unspecific near-infrared dyes in laser-induced fluorescence imaging of experimental arthritis," *Acad. Radiol.* **13**(1), 4–13 (2006).
- M. Eisenblatter et al., "Optical techniques for the molecular imaging of angiogenesis," *Eur. J. Nucl. Med. Mol. Imaging* **37**, S127–S137 (2010).
- A. Wall et al., "Differentiation of angiogenic burden in human cancer xenografts using a perfusion-type optical contrast agent (SIDAG)," *Breast Cancer Res.* **10**(2), R23 (2008).

45. E. S. Izmailova et al., "Use of molecular imaging to quantify response to IKK-2 inhibitor treatment in murine arthritis," *Arthritis Rheum.* **56**(1), 117–128 (2007).
46. A. Wunder et al., "Molecular imaging: novel tools in visualizing rheumatoid arthritis," *Rheumatology* **44**(11), 1341–1349 (2005).
47. A. K. Scheel et al., "Laser imaging techniques for follow-up analysis of joint inflammation in patients with rheumatoid arthritis," *Med. Laser Appl.* **18**, 198–206 (2003).
48. K. G. Hermann et al., "Rheumatoid arthritis of the shoulder joint: comparison of conventional radiography, ultrasound, and dynamic contrast-enhanced magnetic resonance imaging," *Arthritis Rheum.* **48**(12), 3338–3349 (2003).
49. T. A. Carpenter et al., "Visualisation of subchondral erosion in rat monoarticular arthritis by magnetic resonance imaging," *Skeletal Radiol.* **24**(5), 341–349 (1995).
50. T. W. Jamieson et al., "Collagen-induced arthritis in rats. Assessment by serial magnification radiography," *Invest. Radiol.* **20**(3), 324–330 (1985).
51. F. Terrier et al., "Magnetic resonance imaging and spectroscopy of the periarticular inflammatory soft-tissue changes in experimental arthritis of the rat," *Invest. Radiol.* **20**(8), 813–823 (1985).
52. J. M. Stuart, A. S. Townes, and A. H. Kang, "The role of collagen autoimmunity in animal models and human diseases," *J. Invest. Dermatol.* **79**, 121s–127s (1982).
53. D. E. Trentham, "Collagen arthritis as a relevant model for rheumatoid arthritis," *Arthritis Rheum.* **25**(8), 911–916 (1982).
54. D. E. Trentham, A. S. Townes, and A. H. Kang, "Autoimmunity to type II collagen an experimental model of arthritis," *J. Exp. Med.* **146**(3), 857–868 (1977).
55. F. H. Durie, R. A. Fava, and R. J. Noelle, "Collagen-induced arthritis as a model of rheumatoid arthritis," *Clin. Immunol. Immunopathol.* **73**(1), 11–18 (1994).